Computers and Chemical Engineering 95 (2016) 1–9

Contents lists available at ScienceDirect

Computers and Chemical Engineering

journal homepage: www.elsevier.com/locate/compchemeng

Some properties of the GHC equation of state

Angelo Lucia

Department of Chemical Engineering, University of Rhode Island, Kingston, RI 02881, United States

ARTICLE INFO

Article history:
Received 10 March 2016
Received in revised form 26 April 2016
Accepted 4 September 2016
Available online 7 September 2016

Keywords:
Composition functionality of GHC energy parameter
Sensitivity analysis
Second virial coefficients

ABSTRACT

The composition functionality of the mixture energy parameter, a_M, used in the Gibbs-Helmholtz Constrained (GHC) equation of state is studied. An analysis is presented that shows that a_M for liquid mixtures is approximately quadratic in composition. All non-quadratic behavior is due solely to $\ln(T_{cM})$ in the GHC up-scaling equation. If a mean value approximation of this term is used, then $a_M{}^L$ is quadratic, but non-symmetric, in composition. For vapors, non-quadratic behavior is coupled to the molar volume of the mixture through the term $\beta_M = (V_M + b_M)/V_M$. It is shown that the difference between β_M and some average $_{\beta M}$ is very small and $a_M{}^V$ is quadratic in composition. Sensitivity analyses of a_M and resulting molar density to these approximations are also presented. Finally, the non-symmetric composition functionality of a_M is discussed along with GHC predictions of mixture second virial coefficients. Numerical examples are presented to support all claims.

1. Introduction

We begin this article with background and motivation for studying some theoretical properties of the Gibbs-Helmholtz Constrained (GHC) equation of state (Lucia, 2010; Lucia et al., 2012a; Lucia and Bonk, 2012b). In particular, we are interested in the composition functionality of the GHC expression for the mixture energy parameter, a_M, and whether the parameters a_M and b_M in GHC equation satisfy the well known second order virial condition $B_M = b_M - a_M/RT$.

1.1. Background

The GHC equation for the liquid mixture energy parameter (Lucia et al., 2012a) is given by

$$a_M^L = a_M^L(T,p,x) = \left[\frac{a(T_{cM},p_{cM},x)}{T_{cM}} + \frac{b_M U_M^{DL}}{T_{cM} ln2} + \frac{2b_M R ln T_{cM}}{ln2}\right]T - \frac{b_M U_M^{DL}}{ln2} - \left[\frac{2b_M R}{ln2}\right]TlnT \quad (1)$$

where $\frac{a(T_{cM},p_{cM},x)}{T_{cM}} = 0.42748R^2(\frac{T_{cM}}{p_{cM}})$; $b_M = \sum_{i=1}^{C} x_i b_i$, and mixture critical properties satisfy Kay's rules

$$T_{cM} = \sum_{i=1}^{C} x_i T_{ci} \quad (2)$$

$$p_{cM} = \sum_{i=1}^{C} x_i p_{ci} \quad (3)$$

Finally, the internal energy of departure for the mixture, U_M^{DL}, is calculated using a linear mixing rule

$$U_M^{DL} = \sum_{i=1}^{C} x_i U_i^{DL} \quad (4)$$

where U_M^{DL} are pure component internal energies of departure and are a function of T and p only. See Kelly and Lucia (2016) for validation of the mixing rule given by Eq. (4).

1.2. Motivation

The motivation for this work comes from trying to understand the composition functionality of the GHC equation for a_M^L. Plots of a_M^L vs. composition at fixed temperature and pressure appear to show quadratic composition functionality, as illustrated in Fig. 1.

E-mail address: alucia@uri.edu

http://dx.doi.org/10.1016/j.compchemeng.2016.09.004
0098-1354/

Nomenclature

a_M, a_M^L, a_M^V	Mixture energy parameter, for liquid, for vapor
b_M, b_i	Molecular co-volume of mixture, of pure component i
B_M, B_{ij}	Second virial coefficients
c_j, c_{ij}	Coefficients in series approximations of various rational functions
G^E	Excess gibbs free energy
p, p_{cM}, p_{ci}	Pressure, critical pressure of mixture, of pure component i
R	Gas constant
T, T_{cM}, T_{ci}	Temperature, critical temperature of mixture, of pure component i
$U_M^{DL}, U_i^{DL}, U_M^{DV}, U_i^{DV}$	Liquid mixture internal energy of departure, of pure liquid component i, vapor mixture internal energy of departure, of pure vapor component i
V_M, V_i	Molar volume of mixture, of pure component i
x, x_i	Vector of liquid mole fractions, liquid mole fraction of component i
y, y_i	Vector of vapor mole fractions, vapor mole fraction of component i
Greek symbols	
β_M, β_i	Quantity $(V+b)/V$ for mixture and pure components
Δ	Difference or error
ρ_M^L, ρ_M^V	Molar density of liquid mixture, of vapor mixture
Subscripts and superscripts	
c	Critical property
D	Departure function
E	Excess property
i, j	Component index
L	Liquid
M	Mixture
V	Vapor

It is important for the reader to understand that the numerical data (unfilled boxes) shown in Fig. 1 were fit to a second order polynomial using TecPlot 7. Note that the curve for the Soave-Redlich-Kwong (SRK) equation (Soave, 1972) passes directly through the middle of the boxes while the curve for the GHC equation passes through each box but does not go through the middle of each box. This suggests that the functionality of a_M^L for the GHC equation is 'very close' to being quadratic in composition.

1.3. Organization

The remainder of this paper is organized in the following way. Section 2 presents an analysis that shows that a_M^L for the GHC equation is, for all intents and purposes, quadratic in composition and that any deviation from quadratic behavior is due solely to the term lnT_{cM}. This result is first proved for binary mixtures and then generalized for multi-component mixtures. Section 3 relates the GHC equation parameters to second virial coefficients. Section 4 provides some numerical support for the theoretical results established in this paper. Conclusions and a discussion of results are presented in Section 5.

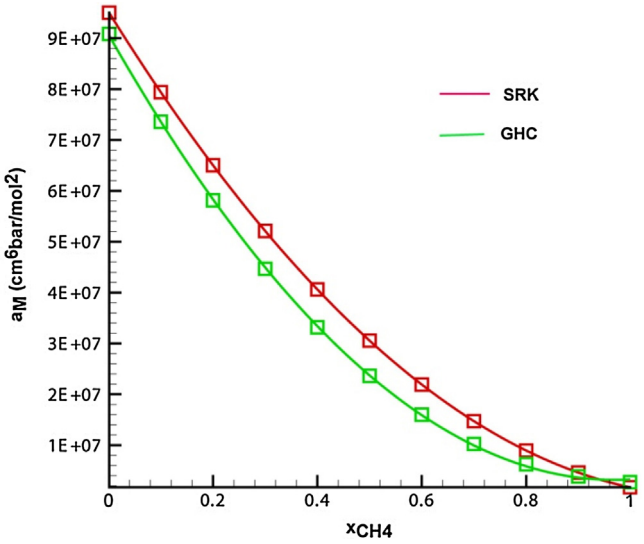

Fig. 1. Composition Functionality of a_M^L for Methane-Decane at 320 K and 10 bar.

2. Composition functionality of the GHC energy parameter for liquid mixtures

The last two terms in Eq. (1) are quadratic and linear in composition respectively because b_M and U_M^{DL} are computed from linear mixing rules; thus they present no difficulties in establishing quadratic composition functionality of $a_M^L(T, p, x)$ at fixed T and p. The challenge in determining the composition functionality of $a_M^L(T, p, x)$ comes from the fact that the terms in square brackets on the right of Eq. (1) are either rational or transcendental functions. The quantity

$$R_1(x) = \frac{T_{cM}}{p_{cM}} = \frac{\sum_{i=1}^{C} x_i T_{ci}}{\sum_{i=1}^{C} x_i p_{ci}} \tag{5}$$

is a rational function in composition as is the term

$$R_2(x) = \frac{b_M}{T_{cM}} = \frac{\sum_{i=1}^{C} x_i b_i}{\sum_{i=1}^{C} x_i T_{ci}} \tag{6}$$

The last term in square brackets involves a transcendental function

$$T(x) = \ln\left(\sum_{i=1}^{C} x_i T_{ci}\right) \tag{7}$$

2.1. Binary liquid mixtures

We start with Kay's rules represented in the form

$$T_{cM} = T_{c2} + (T_{c1} - T_{c2})x_1 \tag{8}$$

$$p_{cM} = p_{c2} + (p_{c1} - p_{c2})x_1 \tag{9}$$

Therefore,

$$R_1(x) = \frac{T_{cM}}{p_{cM}} = \frac{T_{c2} + (T_{c1} - T_{c2})x_1}{p_{c2} + (p_{c1} - p_{c2})x_1} \tag{10}$$

The rational function $R_1(x)$ can also be represented by the infinite series

$$R_1(x_1) = c_0 + c_1 x_1 + c_2 x_1^2 + \ldots \tag{11}$$

Equating the right hand sides of Eqs. (10) and (11) and then multiplying by $p_{c2} + (p_{c1} - p_{c2})x_1$ gives

$$T_{c2} + (T_{c1} - T_{c2})x_1 = [p_{c2} + (p_{c1} - p_{c2})x_1][c_0 + c_1 x_1 + c_2 x_1^2 + \ldots] \tag{12}$$

Expanding the right hand side of Eq. (12) we have

$$T_{c2}+(T_{c1}-T_{c2})x_1=[c_0p_{c2}+c_0(p_{c1}-p_{c2})x_1]+[c_1p_{c2}x_1+c_1(p_{c1}-p_{c2})x_1^2]+[c_2p_{c2}x_1^2+c_2(p_{c1}-p_{c2})x_1^3]+\ldots$$

$$=c_0p_{c2}+[c_0(p_{c1}-p_{c2})+c_1p_{c2}]x_1+[c_1(p_{c1}-p_{c2})+c_2p_{c2}]x_1^2+\ldots \quad (13)$$

Equating coefficients on the left and right of Eq. (13) gives

$$c_0=\frac{T_{c2}}{p_{c2}} \quad (14)$$

$$c_0(p_{c1}-p_{c2})+c_1p_{c2}$$

$$=(T_{c1}-T_{c2})\rightarrow c_1=\left(\frac{(T_{c1}-T_{c2})-(\frac{T_{c2}}{p_{c2}})(p_{c1}-p_{c2})}{p_{c2}}\right) \quad (15)$$

$$c_{j-1}(p_{c1}-p_{c2})+c_jp_{c2}=0, j=2,\ldots,\infty \quad (16)$$

Eqs. (13)–(16) show that the expression

$$R_1(x_1)=c_0+c_1x_1 \quad (17)$$

is exact and therefore $R_1(x_1)$ and the term, $\frac{a(T_{cM},p_{cM},x)}{T_{cM}}=0.42748R^2(\frac{T_{cM}}{p_{cM}})$, in Eq. (1) is linear in composition.

It is also easy to see that $R_2(x_1)$ given by Eq. (6) is an exact linear function in composition by the same analysis. Therefore, the second term in square brackets in Eq. (1), $\frac{b_MU_M^{DL}}{T_{cM}ln2}$, is the inner product of two linear functions in composition, $R_2(x_1)$ and U_M^{DL}, and thus has quadratic composition functionality.

Finally, using a mean value theorem approximation of $\ln(T_{cM})$ gives

$$\ln(T_{cM})=\ln(T_{c2})+[\ln(T_{c1})-\ln(T_{c2})]x_1=x_1\ln(T_{c1})+x_2\ln(T_{c2}) \quad (18)$$

If $\ln(T_{cM})$ in Eq. (1) is replaced by Eq. (18), which can be interpreted as Kay's rule for $\ln(T_{cM})$, then $b_M\ln(T_{cM})$ is quadratic in composition. Alternatively, in Table 1 in Section 4.1 we show that the error in the mean value approximation of $\ln(T_{cM})$ is usually small and thus can be ignored.

Since all terms in Eq. (1) are either linear or quadratic in composition, a_M^L has quadratic composition functionality.

2.2. Multi-component liquid mixtures

The same analysis can be applied to multi-component mixtures, although it is a bit more tedious. That is, using the relationship

$$x_C=1-x_1-x_2-\ldots-x_{C-1} \quad (19)$$

Kay's rules can be written in the form

$$T_{cM}=T_{cC}+(T_{c1}-T_{cC})x_1+(T_{c2}-T_{cC})x_2+\ldots+(T_{cC-1}-T_{cC})x_{C-1} \quad (20)$$

$$p_{cM}=p_{cC}+(p_{c1}-p_{cC})x_1+(p_{c2}-p_{cC})x_2+\ldots+(p_{cC-1}-p_{cC})x_{C-1} \quad (21)$$

As before, there are $C-1$ independent composition variables so

$$R_1(x_1,x_2,\ldots,x_{C-1})=\frac{T_{cM}}{p_{cM}}=\frac{T_{cC}+(T_{c1}-T_{cC})x_1+(T_{c2}-T_{cC})x_2+\ldots+(T_{cC-1}-T_{cC})x_{C-1}}{p_{cC}+(p_{c1}-p_{cC})x_1+(p_{c2}-p_{cC})x_2+\ldots+(p_{cC-1}-p_{cC})x_{C-1}} \quad (22)$$

However, $R_1(x)$ in Eq. (22) can also be represented as an infinite series in the form

$$R(x_1,x_2,\ldots,x_{C-1})=c_{01}+c_{11}x_1+c_{21}x_1^2+\ldots+c_{02}+c_{12}x_2$$

$$+c_{22}x_2^2+\ldots+c_{0C-1}+c_{1C-1}x_{C-1}+c_{2C-1}x_{C-1}^2+\ldots \quad (23)$$

From Eqs. (22) and (23) simple algebraic rearrangement gives

$$T_{cC}+(T_{c1}-T_{cC})x_1+(T_{c2}-T_{cC})x_2+\ldots+(T_{cC-1}-T_{cC})x_{C-1}$$

$$=[p_{cC}+(p_{c1}-p_{cC})x_1+(p_{c2}-p_{cC})x_2+\ldots+(p_{cC-1}-p_{cC})x_{C-1}]$$

$$[c_{01}+c_{11}x_1+c_{21}x_1^2+\ldots+c_{02}+c_{12}x_2+c_{22}x_2^2+\ldots+c_{0C-1}$$

$$+c_{1C-1}x_{C-1}+c_{2C-1}x_{C-1}^2+\ldots] \quad (24)$$

Expanding Eq. (24) and collecting coefficients by component gives a set of linear equations

$$[c_{01}+c_{02}+\ldots+c_{0C-1}]=\frac{T_{cC}}{p_{cC}} \quad (25)$$

$$[c_{01}+c_{02}+\ldots+c_{0C-1}](p_{c1}-p_{cC})+c_{11}p_{cC}=(T_{c1}-T_{cC}) \quad (26)$$

$$[c_{01}+c_{02}+\ldots+c_{0C-1}](p_{c2}-p_{cC})+c_{12}p_{cC}=(T_{c2}-T_{cC}) \quad (27)$$

$$[c_{01}+c_{02}+\ldots+c_{0C-1}](p_{cC-1}-p_{cC})+c_{1C-1}p_{cC}=(T_{cC-1}-T_{cC}) \quad (28)$$

Note from Eq. (24) that all cross terms involving x_ix_j must have coefficients equal to zero. In addition, the coefficients for terms involving higher order powers in composition must also be zero (as before) and therefore all terms involving both x_ix_j for all $i,j=1,\ldots,C-1$ and all x_i^k for all $i=1,\ldots,C-1$ and $k=2,\ldots,\infty$ can be dropped from the analysis.

Eqs. (26)–(28) can be written more compactly in the form

$$[c_0(p_{cj}-p_{cC})+c_{1j}p_{cC}]x_j=(T_{cj}-T_{cC}), j=1,\ldots,C-1 \quad (29)$$

where $c_0=[c_{01}+c_{02}+\ldots+c_{0C-1}]$. Thus Eqs. (25) and (29) give C inhomogeneous linear equations in C unknown coefficients, $c_0, c_{11},\ldots,c_{1C-1}$. Moreover, Eqs. (25) and (29) form a lower triangular system of linear equations whose solution is given by

$$c_0=\frac{T_{cC}}{p_{cC}} \quad (30)$$

$$c_{1j}=\frac{[(T_{cj}-T_{cC})-c_0(p_{cj}-p_{cC})]}{p_{cC}}, j=1,\ldots C-1 \quad (31)$$

Therefore

$$R_1(x_1,x_2,\ldots,x_{C-1})=[c_{01}+c_{02}+\ldots+c_{0C-1}]+c_{11}x_1+c_{12}x_2$$

$$+\ldots+c_{1C-1}x_{C-1} \quad (32)$$

is an exact linear representation of $\frac{T_{cM}}{p_{cM}}$ for a multi-component mixture. Thus the first term in square brackets in Eq. (1) is a linear function in composition.

Using the same analysis, the term $\frac{b_M}{T_{cM}}$ in the second term in square brackets is a linear function in composition. Therefore $\frac{b_MU_M^D}{T_{cM}}$

is quadratic in composition. Finally, the last term in square brackets can be approximated by

$$\ln(T_{cM}) = \sum_{i=1}^{C} x_i \ln(T_{ci}) \tag{33}$$

and $b_M \ln(T_{cM})$ can be approximated by a quadratic function in composition.

As in the binary case, since all terms in Eq. (1) have either linear or quadratic composition functionality, a_M^L is quadratic in composition.

2.3. Vapor mixtures

Eq. (1) is the GHC energy parameter expression for liquid mixtures and is derived using the high pressure limit, $\lim_{p\to\infty} V_M = b_M$ .For vapor mixtures the low pressure limit, $\lim_{p\to 0} V_M \to \infty$, is used and results in a different expression for a_M^V given by

$$a_M^V = a_M^V(T,p,y) = \left[\frac{a(T_{cM},p_{cM},y)}{T_{cM}}\right]T + \left(\frac{T}{T_{cM}} - 1\right)\left[\frac{b_M U_M^{DV}}{ln(\beta_M)}\right] \tag{34}$$

where $U_M^{DV} = -\sum_{i=1}^{C} y_i U_i^{DV}$, $U_i^{DV} = -(\frac{a_i}{b_i})\ln(\beta_i)$, $\beta_i = \frac{V_i+b_i}{V_i}$, and $\beta_M = \frac{V_M+b_M}{V_M}$. See Section 4.1 in Lucia et al. (2012a) for justification of the mixing rule for a_M^V.

If β_M can be approximated by a mean value, say $\bar{\beta}_M$, over the relevant composition range, then the analysis of the composition functionality of a_M^V follows exactly the same analysis as that for a_M^L, only with two fewer terms. This is easily seen by comparing Eqs. (1) and (34). Thus quadratic composition behavior of a_M^V given by Eq. (34) rests solely on the validity of the approximation

$$\beta_{\bar{M}} = \beta_M \tag{35}$$

The magnitude of the difference $\beta_M - \bar{\beta}_M$ for vapor mixtures and the sensitivity of a_M^V and ρ_M^V to this difference will be demonstrated in sub-sections 4.4 and 4.5.

2.4. Asymmetry of a_M^L and a_M^V

The expressions for a_M^L (Eq. (1)) and a_M^V (Eq. (34)) or their respective simplifications all involve the quadratic form

$$b_M U_M^D = \left(\sum_{i=1}^{C} x_i b_i\right)\left(\sum_{j=1}^{C} x_j U_j^D\right) = \sum_{i=1}^{C}\sum_{j=1}^{C} (b_i U_j^D) x_i x_j \tag{36}$$

It is easily seen from Eq. (36) that this quadratic composition term is not symmetric because $b_i U_j^D \neq b_j U_i^D$ for $i \neq j$.

3. GHC EOS parameters and second order virial coefficients

From a virial expansion of the compressibility factor in inverse molar volume, the binomial theorem, and the fact that $b << V$ or $(b_M << V_M)$ for gases, it is easy to show that all of the commonly used cubic EOS satisfy the second order virial coefficient condition given by

$$B_M = b_M - a_M^V/RT \tag{37}$$

which holds for pure components (i.e., $C = 1$) and mixtures. When the parameters of a cubic equation of state provide good approximations to second order virial coefficients, it lends strong statistical credibility to the EOS. Among other things, Eq. (37) validates that the cubic EOS accurately approximates pair-wise interactions of particles in the gas phase.

3.1. Pure components

The pure component form of Eq. (1) is simply the SRK equation with different values of the parameters a and b and therefore satisfies Eq. (37).

3.2. Mixtures

It is well known that the second order virial coefficient for any mixture is quadratic in composition and generally given by

$$B_M = \sum_{i=1}^{C}\sum_{j=1}^{C} y_i y_j B_{ij} \tag{38}$$

See, for example, Reid et al. (p. 79, 1987). Eq. (38) and the facts that the GHC parameters a_M^V and b_M are very weakly quadratic and linear in composition respectively show that second virial coefficient approximations provided by the GHC equation are weak quadratic functions of composition. The primary reason for the weak quadratic functionality of Eq. (34) is due to the fact that the product $b_M U_M^{DV}$ is small because U_M^{DV} is small in magnitude (see Fig. 9 on p. 87 in Lucia et al., 2012a).

4. Numerical support

This section provides quantitative support for the theoretical results in Sections 2 and 3. Numerical results are presented for (1) the difference

$$\Delta \ln(T_{cM}) = \ln(T_{cM}) - \sum_{i=1}^{C} x_i T_{ci} \tag{39}$$

for binary and multi-component liquid mixtures, (2) the sensitivity of a_M^L to $\Delta \ln(T_{cM})$, (3) the sensitivity of GHC predicted liquid molar densities to $\Delta \ln(T_{cM})$, (4) the validity of approximations $\beta_M = \bar{\beta}_M$ for vapor mixtures, (5) the sensitivity of a_M^V and ρ_M^V to differences

$$\Delta\beta_M = \beta_M - \bar{\beta}_M \tag{40}$$

and (6) GHC predictions of second virial coefficients. All numerical results were performed on a Dell Inspiron laptop with the LF95 compiler. Critical properties and molecular co-volumes for all components used in the numerical examples are given in Table A1 in Appendix A. Pure component internal energies of departure are given in Table A2. Finally many of the numerical results are reported as AAD% differences instead of AAD% errors since the measures involve a pair of numerical results.

4.1. Mean Value Approximations of $\ln(T_{cM})$

Table 1 gives Average Absolute Deviation Percent (AAD%) differences and maximum differences in Eq. (39), where T_{cM} is given by Kay's rule. One hundred (100) and 4950 points throughout the composition space were sampled for binary and ternary mixtures respectively.

There are two points to note about the results shown in Table 1

1. Larger differences in component critical temperatures result in larger AAD% differences $\Delta\ln(T_{cM})$. For example, the relatively low critical temperature of methane compared to other hydro-

Table 1
Differences in $\Delta \ln(T_{cM}) = \ln(T_{cM}) - \sum_{i=1}^{C} x_i T_{ci}$.

No.	Mixture	AAD% Difference[a]	Maximum Difference
1	CH_4-ethane	0.33	0.51
2	CH_4-octane	1.65	2.52
3	CH_4-hexadecane	2.36	3.63
4	CH_4-triacontane	2.95	4.53
5	CH_4-benzene	1.62	2.47
6	CH_4-water	2.02	3.10
7	CO_2-methane	0.33	0.50
8	CO_2-ethane	2.24×10^{-5}	3.39×10^{-5}
9	CO_2-octane	0.53	0.81
10	CO_2-hexadecane	0.98	1.50
11	CO_2-triacontane	1.35	2.07
12	CO_2-benzene	0.51	0.78
13	CO_2-water	0.76	1.16
14	ethane-water	0.75	1.14
15	octane-water	0.02	0.03
16	hexadecane-water	0.015	0.023
17	triacontane-water	0.09	0.14
18	benzene-water	0.03	0.04
19	CH_4-octane-hexadecane	1.87	3.63
20	CH_4-octane-water	1.68	3.10
21	CH_4-benzene-hexadecane	1.87	3.63
22	CH_4-benzene-water	1.67	3.10
23	CO_2-octane-hexadecane	0.78	1.50
24	CO_2-octane-water	0.63	1.16
25	CO_2-benzene-hexadecane	0.76	1.50
26	CO_2-benzene-water	0.63	1.16
27	CO_2-hexadecane-water	0.82	1.48

[a] $\text{AD\%} = 100|\ln(T_{cM}) - \sum_{i=1}^{C} x_i \ln(T_{ci})|/\ln(T_{cM})$.

carbons and water results in larger AAD% differences $\Delta\ln(T_{cM})$ for mixtures containing methane.

2. For the ternary mixtures studied, the AAD% differences $\Delta\ln(T_{cM})$ for mixtures that differ only by benzene and octane (.e.g., mixtures 19 and 21; 20 and 22; 23 and 25; 24 and 26) are essentially the same because the critical temperatures of benzene and octane are almost the same ($T_{c,benzene} = 562.16$ K and $T_{c,octane} = 568.80$ K).

4.2. Sensitivity of a_M^L to Errors in $\ln(T_{cM})$

It is important to quantify the effect of using mean value approximations of $\ln(T_{cM})$ in the expression for a_M^L and the resulting liquid molar density computed by the GHC equation. From Eq. (1), it is easily seen that

$$\frac{\partial a_M^L}{\partial \ln(T_{cM})} = \frac{2b_M RT}{ln2} \tag{41}$$

and that the error in $\ln(T_{cM})$ of interest here is the difference between the actual value of $\ln(T_{cM})$ and the mean value approximation given by Eq. (33). That is,

$$\Delta \ln(T_{cM}) = \ln(T_{cM}) - \sum_{i=1}^{C} x_i \ln(T_{ci}) \tag{42}$$

The corresponding change in the liquid mixture energy parameter is

$$\Delta a_M^L = \left(\frac{2b_M RT}{ln2}\right)\left[\ln(T_{cM}) - \sum_{i=1}^{C} x_i \ln(T_{ci})\right] = \left(\frac{2b_M RT}{ln2}\right)\Delta \ln(T_{cM}) \tag{43}$$

The relatively small differences shown in Table 1 suggests that a_M^L is insensitive to mean value approximations of $\ln(T_{cM})$ and this is clearly supported by Fig. 2, which gives plots of $100|\Delta a_M^L|/a_M^L$, vs. composition for a number of binary liquid mixtures, where Δa_M^L is given by Eq. (43). Statistical results are shown in Table 2, irrespective of whether the fluid was single liquid or supercritical fluid and whether single liquid was materially stable or unstable. High pressure and relatively low temperature conditions were selected to ensure real liquid or liquid-like supercritical fluid behavior. Table 2 also shows the AAD% differences in Δa_M^L for each mixture.

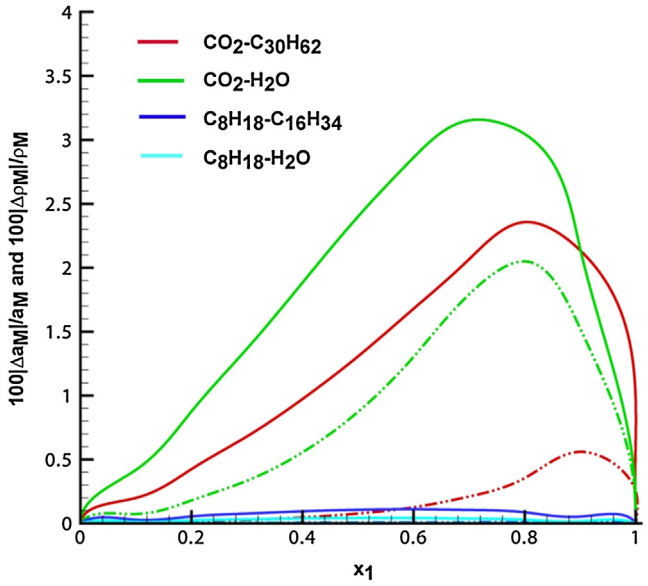

Fig. 2. Sensitivity of GHC Liquid Mixture Energy Parameter and Liquid Mixture Molar Density.
(a) $100|\Delta a_M^L|/a_M^L$ (solid curves); (b) $100|\Delta \rho_M^L|/\rho_M^L$ (dot-dash curves).

Table 2
Mixture Specifications and AAD% Differences Δa_M^L.

Mixture	T (K)	p (bar)	AAD% Error in Δa_M^L [a]
CO_2-triacontane	300	200	1.11
CO_2-water	373.15	400	1.68
octane-hexadecane	350	300	0.07
octane-water	323.15	500	0.025

[a] AD% differences = $100|\Delta a_M^L|/a_M^L$.

Note that the AAD% differences in Δa_M^L are directly proportional to the corresponding differences $\Delta\ln(T_{cM})$, as shown by Eq. (42). So, for example, the small error in Δa_M^L for a non-ideal mixture like octane-water is supported by the maximum difference $\Delta\ln(T_{cM})$ of 0.03, as shown in Table 1. Also note that the maximum difference in the mixture energy parameter is 3%.

4.3. Sensitivity of Liquid Molar Density to Differences $\Delta\ln(T_{cM})$

Since a_M^L is relatively insensitive to differences resulting from mean value approximations of $\ln(T_{cM})$, it is easily shown that liquid molar density is also insensitive to $\Delta\ln(T_{cM})$. The sensitivity of binary liquid mixture molar density to mean value approximations of $\ln(T_{cM})$ are also shown in Fig. 2 over the entire composition range. As in sub-Section 4.2, Table 3 gives the conditions for each mixture and the AAD% difference in liquid mixture molar density.

As expected, Fig. 2 and Table 3 show that the sensitivity of liquid mixture molar density is quite small and all under 1% for the mixtures studied.

Table 3
Mixture Specifications and AAD% Difference in ρ_M^L.

Mixture	T (K)	p (bar)	AAD% $\Delta\rho_M^L$ [a]
CO_2-triacontane	300	200	0.15
CO_2-water	373.15	400	0.81
octane-hexadecane	350	300	0.005
octane-water	323.15	500	0.003

[a] AD% difference = $100|\Delta\rho_M^L|/\rho_M^L$.

Table 4 provides an example of the impact of $\ln(T_{cM})$ on the density of CO_2-water mixtures and compares those density results to density predictions for the volume translated SRK (SRK+) equation (Peneloux et al., 1982), the predictive SRK (PSRK) equation of Holderbaum and Gmehling (1991), and experimental data given in Teng et al. (1997).

Our implementations of these three equations of state all use the Soave form of the Redlich-Kwong equation, a linear mixing rule for b_M, and are predictive (not correlated to any data). The only difference between them is the way in which a_M^L is computed. The SRK+ equation uses a quadratic mixing rule and geometric combining rule for a_M^L with $k_{12} = 0$ while the PSRK equation uses the UNIFAC group contribution method to estimate the excess Gibbs free energy and a G^E −based mixing rule for a_M^L. Thus the comparisons that are presented in Table 4 represents, in our opinion, a true test of the impact of the GHC up-scaling equation for a_M^L (i.e., Eq. (1)) on liquid density predictions. All density computations were converged to $||f(z)|| \leq 10^{-12}$, where $f(z)$ is the cubic polynomial in compressibility factor for each equation of state.

Note that the GHC equation with either a_M^L computed using Eq. (1) or a_M^L computed using mean value approximations of $\ln(T_{cM})$ have virtually the same as well as the lowest AAD% error in mass density. Also, the differences in the densities for the two implementations of the GHC equation are small because the CO_2 mole fraction in the aqueous phase is small (i.e., in the range [0.0250, 0.0349]). Surprisingly, the GHC implementation using mean value approximations of $\ln(T_{cM})$ performs ever so slightly better than the implementation using Eq. (1).

Table 5
Vapor Mixture Conditions and AAD% Errors[a].

Mixture	T (K)	p (bar)	composition	$\bar{\beta}_M$	AAD% error
CH_4-octane	500	10	[0,1]	1.02348	1.01
CH_4-CO_2	400	30	[0,1]	1.02794	0.0023
CO_2-ethane	350	40	[0,1]	1.06446	0.960
CO_2-decane	600	5	[0,1]	1.01088	0.452
CO_2-water	473.15	300	[0.845, 1]	1.28285	0.614
ethane-water	523.15	200	[0.72,1]	1.20757	1.71
benzene-water	573.15	50	[0,1]	1.09040	3.61

[a] AD% error = $100|\beta_M - \bar{\beta}_M|/\beta_M$.

4.4. Validity of the Approximations $\beta_M = \bar{\beta}_M$ for Vapor Mixtures

Quadratic composition functionality of a_M^V given by Eq. (34) can only be established if the approximation $\beta_M = \bar{\beta}_M$ is valid over the composition range of interest. Table 5 gives values of $\bar{\beta}_M$ and AAD% differences for a number of binary vapor mixtures where the temperatures, pressures, and composition ranges listed in Table 5 were chosen to ensure real vapor phase behavior.

As expected, the AAD% differences in the approximation given by Eq. (35) is reasonably small (<4%) – even under high temperature and high pressure conditions. In particular, for CO_2-water, the vapor phase covers the composition region $x_{CO2} \in [0.8, 1]$ and is actually supercritical vapor; see Fig. 2, p. 1061 in Takenouchi and Kennedy (1964) . Ethane-water at high temperature and pressure exhibits an AAD% error that is somewhat higher (1.71%) but again the vapor is supercritical vapor in the relevant composition range. Finally, the worse case is benzene-water at high temperature where the AAD% difference is 3.61%.

4.5. Sensitivity of a_M^V and ρ_M^V to the approximation $\beta_M = \bar{\beta}_M$

In this sub-section, the sensitivity of a_M^V and ρ_M^V to the approximation $\beta_M = \bar{\beta}_M$ is quantified. The impact of the difference, $\Delta\beta_M = \beta_M - \bar{\beta}_M$, on the vapor energy parameter, a_M^V, and vapor

Table 4
Mass Densities of CO_2-Water Mixtures.

T (K)	p (bar)	x_{CO2}	ρ(kg/m^3)				
			SRK+	PSRK	GHC	GHC[a]	Teng et al.
278	64.4	0.0293	1047.43	1049.31	1030.52	1030.45	1018.10
	98.7	0.0308	1048.58	1050.49	1031.62	1031.55	1019.77
	147.7	0.0320	1049.89	1051.83	1032.62	1032.63	1020.63
	196.8	0.0331	1051.16	1053.13	1033.71	1033.64	1022.01
	245.8	0.0341	1052.38	1054.37	1034.61	1034.54	1023.33
	294.9	0.0349	1054.54	1055.54	1035.38	1035.31	1025.33
283	64.4	0.0279	1042.31	1044.12	1026.97	1026.90	1016.97
	98.7	0.0294	1043.30	1045.32	1028.11	1028.02	1018.60
	147.7	0.0305	1044.77	1046.65	1029.13	1029.05	1019.40
	196.8	0.0316	1046.07	1047.97	1030.15	1030.07	1020.75
	245.8	0.0326	1047.33	1049.25	1031.06	1030.98	1021.70
	294.9	0.0334	1048.51	1050.45	1031.86	1031.76	1023.98
288	64.4	0.0269	1037.25	1039.01	1023.56	1023.47	1015.75
	98.7	0.0280	1038.30	1040.09	1024.54	1024.46	1017.10
	147.7	0.0296	1039.79	1041.63	1025.88	1025.79	1018.22
	196.8	0.0309	1041.18	1043.05	1027.02	1026.94	1019.68
	245.8	0.0319	1042.47	1044.36	1027.95	1027.86	1020.96
	294.9	0.0327	1043.69	1045.59	1028.75	1028.65	1022.87
293	64.4	0.0250	1031.85	1033.53	1019.66	1019.59	1013.68
	98.7	0.0258	1032.81	1034.52	1020.46	1020.38	1014.80
	147.7	0.0275	1034.37	1036.12	1021.86	1021.79	1015.97
	196.8	0.0293	1035.95	1037.75	1023.33	1023.25	1017.72
	245.8	0.0304	1037.31	1039.13	1024.32	1024.23	1019.05
	294.9	0.0312	1038.55	1040.39	1025.12	1025.03	1019.79
AAD%[b]			2.30	2.49	0.83	0.82	

[a] With mean value approximations of $\ln(T_{cM})$ given by Eq. (33).
[b] AD% error = $100|\rho^{exp} - \rho^{calc}|/\rho^{exp}$.

Table 6
Sensitivity of a_M^V and ρ_M^V to the Approximation $\beta_M = \bar{\beta}_M$.

Mixture	T (K)	p (bar)	composition	AAD% Error in a_M^V [a]	AAD% Error in ρ_M^V [b]
CH_4-octane	500	10	[0,1]	2.48×10^{-4}	7.71×10^{-6}
CH_4—CO_2	400	30	[0,1]	5.59×10^{-7}	4.59×10^{-8}
CO_2-ethane	350	40	[0,1]	1.39×10^{-5}	5.68×10^{-6}
CO_2-decane	600	5	[0,1]	1.09×10^{-4}	1.82×10^{-6}
CO_2-water	473.15	300	[0.845, 1]	5.54×10^{-6}	6.67×10^{-6}
ethane-water	523.15	200	[0.72,1]	1.55×10^{-5}	1.19×10^{-5}
benzene-water	573.15	50	[0,1]	1.07×10^{-5}	3.79×10^{-6}

[a] AD% error = $100|\Delta a_M^V|/a_M^V$; [b] AD% error = $100|\Delta \rho_M^V|/\rho_M^V$.

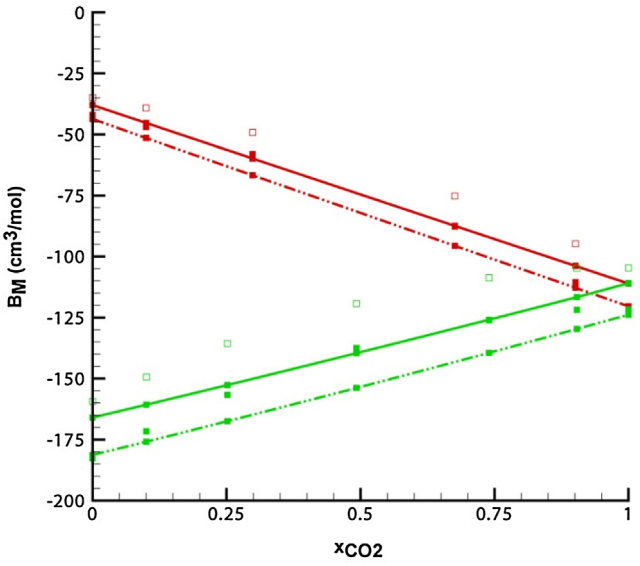

Fig. 3. Mixture Second Virial Coefficients Predicted by Multi-Scale GHC Equation. Red squares (Brugge et al., 1989 CO_2-CH_4, filled = 300 K, unfilled = 320 K). Green squares (Brugge et al., 1989 CO_2-ethane, filled = 300 K, unfilled = 320 K).

molar density, ρ_M^V depends strongly on the partial derivative. However, Eq. (34) and the fact that

$$U_M^{DV} \approx -\left(\frac{a_M}{b_M}\right) \ln(\beta_M) \tag{44}$$

as shown in Eq. (19) on p. 87 of Lucia et al. (2012a) gives

$$a_M^V = \frac{[\frac{a(T_{cM}, p_{cM}, y)}{T_{cM}}]T}{(\frac{T}{T_{cM}} - 1)} \tag{45}$$

which shows that the derivative of a_M^V with respect to $\ln(\beta_M)$ is zero. Therefore, the relative difference in the vapor mixture energy parameter, $\Delta a_M^V/a_M^V$, is given by

$$\Delta a_M^V/a_M^V \approx 0 \tag{46}$$

Table 6 clearly shows that there is no question that the approximation $\beta_M = \bar{\beta}_M$ is valid for vapor phases and has absolutely no impact on a_M^V and ρ_M^V regardless of conditions (i.e., high or low temperature, high or low pressure). This means that $\beta_M = \bar{\beta}_M$ has no impact on vapor phase partial fugacity coefficients.

4.6. GHC predictions of second virial coefficients

In this sub-section, second virial coefficients for CH_4-CO_2 and CO_2-ethane over a range of compositions at 300 and 320 K were computed using Eq. (37), where a_M and b_M were determined by the multi-scale GHC approach and compared to experimental values of B_M defined by Eq. (38) (see Table XI, p. 402 in Brugge et al., 1989). Fig. 3 shows the results of this comparison.

Note that the plots in Fig. 3 show that GHC predictions of mixture second virial coefficients exhibit the correct trends with respect to temperature and composition; however, the composition functionality is linear. This is easily explained using the analysis of the vapor phase expression for a_M^V (i.e., Eq. (34)). Note that the first term on the right of Eq. (34) is linear in composition and while the second term, $b_M U_M^{DV}$, is theoretically quadratic in composition, it is very small in comparison (i.e., many orders of magnitude less). As a result, second virial coefficients for the GHC equation computed using Eq. (37) are essentially linear in composition.

The real question regarding the linear composition functionality of GHC predictions of mixture second virial coefficients is – does it matter in practice? To answer this question, GHC vapor mixture molar density predictions are compared to those for the SRK equation with and without a binary interaction parameter (k_{ij}), and the truncated virial equation used by Brugge et al. (p. 401, 1989) given by

$$z = 1 + B\rho + C\rho^2 \tag{47}$$

Results for vapor molar density of CO_2-ethane mixtures at 300 K are shown in Table 7. Temperatures, pressures, compositions, and virial equation density data shown in that table were taken directly from Brugge et al. (Table IX, p.397–399).

When compared to molar densities for the truncated virial equation at 300 K reported by Brugge et al. (1989), calculated densities for the GHC equation and SRK equation with $k_{ij} = 0$ are comparable, but both show greater error than densities computed with the SRK equation and $k_{ij} = 0.1363$. AAD% errors in SRK molar densities with $k_{ij} = 0$ and GHC molar densities were 1.28% and 1.33 respectively and suggest that errors in GHC second virial coefficients do not have any significant impact on vapor density in practice.

5. Conclusions and discussion

The composition functionality of liquid and vapor mixture energy parameters given by the GHC equation of state were rigorously analyzed. It was shown that both expressions for the mixture energy parameter are quadratic, but non-symmetric, in composition under very reasonable approximations. For liquid mixtures, when $\ln(T_{cM})$ was replaced by $\sum_{i=1}^{C} x_i \ln(T_{ci})$, the resulting difference was small (<4%) and the corresponding sensitivity of a_M^L and ρ_M^L over the entire binary composition range were <2% and <1% respectively for all mixtures studied. The maximum differences in a_M^L and ρ_M^L were 3.15% and 1.79% for mixtures of CO_2-water at 100 °C and 400 bar. In contrast, for vapor mixtures, the approximation of $\beta_M = (V_M + b_M)/V_M$ by an average value, $\bar{\beta}_M$, provided rigorous, but weak, quadratic composition functionality of a_M^V. Moreover, this vapor approximation, $\bar{\beta}_M$, resulted in AAD% differences in a_M^V and ρ_M^V of $<10^{-3}$ and $<10^{-4}$ respectively for all mixtures studied. Finally, although second virial coefficients predicted by the GHC equation exhibited weak quadratic composition functionality, this did not have an impact of vapor density predictions.

Table 7
Vapor Molar Densities of CO_2-Ethane Using the SRK, GHC, and Virial Equations.

T^{exp} (K)[a]	x_{CO2}[a]	p^{exp} (bar)[a]	ρ (mol/m^3)			
			SRK	SRK[b]	GHC	Virial[a]
299.995	0.10043	33.6149	1924.32	1851.66	1902.78	1897.17
299.984		8.4312	360.469	359.80	360.118	359.798
300.030		1.6826	68.271	68.249	68.260	68.232
300.008		23.8378	1185.48	1175.92	1179.94	1177.23
300.049		11.6983	514.072	512.653	513.32	512.668
299.997	0.25166	37.8660	2249.47	2150.09	2237.74	2161.22
300.013		20.1993	951.859	940.474	950.85	941.259
300.011		1.9161	77.819	77.760	77.815	77.749
299.996		14.0379	625.403	620.10	625.029	621.170
299.986		10.4195	450.603	448.409	450.424	448.498
299.984	0.49245	31.9369	1656.96	1603.49	1661.12	1605.68
300.006		15.8353	707.231	699.700	707.754	699.844
299.999		7.2941	306.323	305.046	306.407	305.024
300.004		3.2558	133.180	132.948	133.197	132.942
299.976		42.9001	2594.61	2421.71	2610.55	2432.12
300.005	0.73978	43.0433	2434.43	2328.97	2454.19	2342.95
300.006		22.3347	1032.41	1019.25	1034.19	1020.68
299.988		26.5773	1270.58	1249.46	1273.59	1251.76
300.007		8.5746	361.100	359.726	361.261	359.907
299.993		2.5485	103.622	103.516	103.634	103.478
299.990	0.90367	36.7186	1879.48	1855.14	1885.47	1859.26
299.991		12.4919	536.143	534.720	536.343	534.747
299.986		50.7547	3047.92	2957.83	3080.39	2976.68
299.986		19.2142	859.806	855.865	860.455	856.150
300.013		5.9598	246.491	246.209	246.525	246.232
AAD%[c]			1.28	0.23	1.33	

[a] Temperatures, pressures, compositions, and molar densities as reported by Brugge et al. (1989) .
[b] $k_{12} = 0.1363$.
[c] $AAD\% = 100|\rho^{virial} - \rho^{EOS}|/\rho^{virial}$.

Given that the GHC equation is purely predictive and provides considerably better molar densities than other cubic EOS in the van der Waals family for

1 Pure liquids (see, Table 14, p. 1756 in Lucia and Henley, 2013).
2 Liquid mixtures including aqueous electrolytes (see, Table 6 in Lucia et al., 2012a).
3 Other condensed phases such as hexagonal ice and gas hydrates (see Tables 2 and 5 in Henley et al., 2014).

small AAD% errors in vapor density are, in our opinion, acceptable.

Finally, the analysis and numerical results in this article suggest a number of possible ways of improving the multi-scale GHC equation and some interesting open questions, including

1 The use of alternate expressions for the GHC equation energy parameters a_M^L and a_M^V using the approximations $\sum_{i=1}^{C} x_i \ln(T_{ci})$ and $\tilde{\beta}_M$ respectively.
2 Finding better estimates of U_i^D in order to provide stronger quadratic composition functionality of a_M^V.
3 Is it necessary for the mixture energy parameter to be symmetric in composition? With regard to this last point, the usual polynomial mixing rule for the mixture energy parameter is symmetric and quadratic (see, for example, Eqs. (11) and (13), p. 53 in Walas, 1985) when the binary interaction parameters, k_{ij}, are zero. However, if $k_{ij} \neq 0$, which is quite often the case in practice, then the usual polynomial mixing rules are asymmetric. Some G^E –based mixing rules such as the Wong-Sandler mixing rule are symmetric because they invoke the boundary condition given by Eq. (37) (see, Eqs. (7)– (10)–(3) in Sandler, 1999) while others like the one used in the implementation of the PSRK equation (Gmehling, 2003).

$$a_M = b_M RT\left[\sum_{i=1}^{C}\frac{a_i x_i}{b_i RT} + \frac{G_0^E/RT + \sum_{i=1}^{C}\ln(b_M/b_i)x_i}{\ln(1.1/2.1)}\right] \tag{48}$$

are non-symmetric. Symmetry in energy parameter mixing rules has never been justified while the quadratic composition functionality affords cubic EOS like the SRK equation with some statistical thermodynamic support (see Eqs. (37) and (38)). In contrast, the GHC energy parameter expression is non-symmetric and, a_M^V in particular, is only very weakly quadratic in composition—so it does not do well in matching second virial coefficients. Nevertheless, the GHC equation density predictions are clearly better than many commonly used cubic EOS like the SRK and Peng-Robinson equations with and without volume translation over a very wide range of fluids (spherical, non-spherical, polar, non-polar, long chain, aromatic, and so on).

Appendix A.

Critical Properties and Molecular Co-volumes for Pure Components.

Table A1 gives the critical properties (T_c, p_c, ω, z_c) and molecular co-volume (b) for all components used throughout this article.

Table A1
Pure Component Critical Properties and Molecular Co-volumes.

Species	T_c (K)	p_c (bar)	ω	z_c	b(cm^3/mol)
methane	190.53	46.03	0.011	0.288	29.614
CO_2	304.20	73.80	0.224	0.274	28.169
ethane	305.40	48.83	0.099	0.285	46.127
octane	568.80	24.90	0.397	0.259	143.145
hexadecane	722.11	16.84	0.637	0.224	283.040
triacontane	848.68	7.40	0.938	0.206	524.561
benzene	562.16	48.98	0.210	0.271	76.354
water	647.37	221.20	0.345	0.233	16.363

References

Brugge, H.B., Hwang, C.A., Rogers, W.J., Holste, J.C., Hall, K.R., Lemming, W., Esper, G.J., Marsh, K.N., Gammon, B.E., 1989. Experimental cross virial coefficients for binary mixtures of carbon dioxide with nitrogen, methane, and ethane at 300 and 320 K. Phys. A 156, 382–416.

Gmehling, J., 2003. Potential of group contribution methods for the prediction of phase equilibria and excess properties of complex mixtures. Pure Appl. Chem. 75, 875–888.

Henley, H., Thomas, E., Lucia, A., 2014. Density and phase equilibrium for ice and structure I hydrates using the Gibbs-Helmholtz constrained equation of state. Chem. Eng. Res. Des. 92, 1977–1991.

Holderbaum, T., Gmehling, J., 1991. PSRK: A group contribution equation of state based on UNIFAC. Fluid Phase Equilib. 70, 251–265.

Kelly, R.B., Lucia, A., 2016. On the linear approximation of mixture internal energies of departure. Comput. Chem. Eng. 85, 72–75.

Lucia, A., Bonk, B.M., 2012b. Molecular geometry effects and the Gibbs? Helmholtz Constrained equation of state. Comput. Chem. Eng. 37, 1–14.

Lucia, A., Henley, H., 2013. Thermodynamic consistency of the multi-scale Gibbs-Helmholtz constrained equation of state. Chem. Eng. Res. Des. 91, 1748–1759.

Lucia, A., Bonk, B.M., Waterman, R.R., Roy, A., 2012a. A multi-scale framework for multi-phase equilibrium flash. Comput. Chem. Eng. 36, 79–98.

Lucia, A., 2010. A multi-scale Gibbs-Helmholtz constrained cubic equation of state. J. Thermodyn. (article id: 238365).

Peneloux, A., Rauzy, E., Freze, R., 1982. A consistent correction for Redlich-Kwong-Soave volumes. Fluid Phase Equilib. 8, 7–23.

Reid, R.C., Prausnitz, J.M., Poling, B.E., 1987. The Properties of Gases and Liquids, 4th Ed. McGraw-Hill, Inc., New York.

Sandler, S.I., 1999. Chemical and Engineering Thermodynamics, 3rd Ed. John Wiley & Sons, Inc, New York, NY.

Soave, G., 1972. Equilibrium constants from a modified Redlich-Kwong equation of state. Chem. Eng. Sci. 27, 1197–1203.

Takenouchi, S., Kennedy, G.C., 1964. The binary system H2O-CO2 at high temperatures and pressures. Am. J. Sci. 262, 1055–1074.

TecPlot7 User's Manual. Amtec Engineering, Inc. Bellevue, WA.

Teng, H., Yamasaki, A., Chun, M.K., Lee, H., 1997. Solubility of liquid CO2 in water at temperatures from 278 to 293 and pressures from 64.4 MPa to 29.49 MPa and densities of the corresponding aqueous phase. J. Chem. Thermodyn. 29, 1301–1310.

Walas, S.M., 1985. Phase Equilibria in Chemical Engineering. Butterworth Publishers, Stoneham, MA.